Journal of General Virology (2004), **85**, 1039–1048 DOI 10.1099/vir.0.19687-0

Compatibility of the movement protein and the coat protein of cucumoviruses is required for cell-to-cell movement

Katalin Salánki,[1] Ákos Gellért,[1,2] Emese Huppert,[1] Gábor Náray-Szabó[3] and Ervin Balázs[1]

[1]Agricultural Biotechnology Center, Szent-Györgyi Albert u. 4, H-2100 Gödöllő, Hungary

[2]Department of Theoretical Chemistry, Eötvös Loránd University, Pázmány Péter Sétány 1/A, H-1117 Budapest, Hungary

[3]Protein Modelling Group, Hungarian Academy of Sciences – Eötvös Lóránd University, Pázmány Péter Sétány 1/A, H-1117 Budapest, Hungary

Correspondence
Katalin Salánki
salanki@abc.hu

For the cell-to-cell movement of cucumoviruses both the movement protein (MP) and the coat protein (CP) are required. These are not reversibly exchangeable between *Cucumber mosaic virus* (CMV) and *Tomato aspermy virus* (TAV). The MP of CMV is able to function with the TAV CP (chimera RT), but TAV MP is unable to promote the cell-to-cell movement in the presence of CMV CP (chimera TR). To gain further insight into the non-infectious nature of the TR recombinant, RNA 3 chimeras were constructed with recombinant MPs and CPs. The chimeric MP and one of the CP recombinants were infectious. The other recombinant CP enabled virus movement only after the introduction of two point mutations (Glu→Lys and Lys→Arg at aa 62 and 65, respectively). The mutations served to correct the CP surface electrostatic potential that was altered by the recombination. The infectivity of the TR virus on different test plants was restored by replacing the sequence encoding the C-terminal 29 aa of the MP with the corresponding sequence of the CMV MP gene or by exchanging the sequence encoding the C-terminal 15 aa of the CP with the same region of TAV. The analysis of the recombinant clones suggests a requirement for compatibility between the C-terminal 29 aa of the MP and the C-terminal two-thirds of the CP for cell-to-cell movement of cucumoviruses.

Received 1 October 2003
Accepted 28 November 2003

INTRODUCTION

To infect host plants successfully, viruses must be able to spread from the initially infected cell to the neighbouring cells through plasmodesmata (cell-to-cell movement) until reaching the phloem for rapid invasion of distant plant parts (long-distance movement). The cell-to-cell movement requires viral movement proteins (MPs), which mediate the transport of viral genomes through plasmodesmata. In several cases, the presence of MP is sufficient for virus cell-to-cell movement and the virus moves as a ribonucleoprotein complex (e.g. *Tobacco mosaic virus*, TMV). In other cases, the coat protein (CP) is also necessary for this process; tubular structures are formed that traverse the cell wall through modified plasmodesmata (e.g. tospoviruses, comoviruses and nepoviruses) and the virus moves as a virus particle (reviewed by Carrington *et al.*, 1996; Lazarowitz & Beachy, 1999). Cucumoviruses also require the presence of the CP for cell-to-cell movement, but not the assembly of virus particles (Kaplan *et al.*, 1998).

Cucumoviruses [*Cucumber mosaic virus* (CMV), *Tomato aspermy virus* (TAV) and *Peanut stunt virus* (PSV)] have single-stranded, positive-sense, functionally divided RNA genomes consisting of three genomic RNAs. Proteins 1a and 2a encoded by RNA 1 and 2, respectively, have been demonstrated to be involved in viral RNA replication (Nitta *et al.*, 1988). RNA 2 also encodes a small protein called 2b, which affects the virulence of the virus (Ding *et al.*, 1996; Soards *et al.*, 2002), can suppress the initiation of RNA silencing (Béclin *et al.*, 1998; Brigneti *et al.*, 1998) and has a role in promoting cell-to-cell movement (Shi *et al.*, 2003). Both proteins encoded by RNA 3, the 3a protein and the CP, have been shown to be indispensable for virus transport (Suzuki *et al.*, 1991). The 3a protein was shown to function as the MP of cucumoviruses; it has sequence and functional similarity to the MP of TMV (Melcher, 1990; Kaplan *et al.*, 1995), traffics itself and viral RNA from cell to cell (Ding *et al.*, 1995), binds single-stranded RNA (Li & Palukaitis, 1996) and associates with the cell wall, both in infected plants and in transgenic plants expressing the CMV 3a gene (Vaquero *et al.*, 1994, 1996; Cooper & Dodds, 1995). The RNA-binding domain of the CMV MP has been localized between amino acids (aa) 174 and 233 (Vaquero *et al.*, 1997), and the C-terminal

33 aa of the MP were shown to be responsible for specificity to the viral genome during cell-to-cell movement (Nagano *et al.*, 1997). The functional domains of the MP have been analysed in detail (Li *et al.*, 2001), while the precise role of the CP in cell-to-cell movement is still not known. The N-terminal proximal part of the CP can be deleted without abolishing cell-to-cell movement of the virus, but in this case the formation of stable virions did not occur (Kaplan *et al.*, 1998; Schmitz & Rao, 1998).

The MP of CMV can be replaced with the MP of unrelated viruses resulting in viable hybrid viruses, as was shown for the MP of *Groundnut rosette virus* (Ryabov *et al.*, 1999) and *Cymbidium ringspot virus* (Huppert *et al.*, 2002). In these cases, the hybrid virus was able to move from cell to cell, even in the absence of the CP.

Our previous results have shown that not all combinations of the MP and CP of R-CMV and P-TAV are infectious. While the recombinant RNA 3 with the MP of CMV and the CP of TAV (chimera RT) caused systemic infection in different host plants, the reverse construct with the MP of TAV and the CP of CMV (chimera TR) was not infectious in the presence of R-CMV RNAs 1 and 2 in plants, even though it replicated in tobacco protoplasts (Salánki *et al.*, 1997). In the present study, we analysed the MP and CP regions responsible for movement deficiency of the TR chimera.

METHODS

Plasmid constructs. Construction of the cDNA clones of P-TAV RNA 3, pT3 (Salánki *et al.*, 1994), and R-CMV, pR1, pR2 and pR3, the mutant pT3/*Nde*I, pR3/*Nde*I and chimeras pRT and pTR has been described previously (Salánki *et al.*, 1997). To facilitate further cloning steps, restriction endonuclease recognition sites were introduced to different clones by PCR-directed mutagenesis. Clone pT3/BN was generated by incorporating a *Bam*HI restriction site into pT3/*Nde*I at nt 825–830. An *Spe*I restriction site was introduced into both pT3/*Nde*I and pR3/*Nde*I at nt 1338–1443, resulting in the clones pT3/NS and pR3/NS, respectively. The nucleotide sequences of the mutated DNAs were confirmed by DNA sequencing. The cloning steps were carried out by standard procedures (Sambrook *et al.*, 1989).

For the construction of MP chimeras, the C-terminal region of the MP of pR3 was PCR amplified using primers 5′-GGGATCCGAGTCCGAGATTTTAAACGAA-3′ (the *Bam*HI site is underlined) and 5′-**ATACACGTATATATATAACAACAGGC**CTAAAGACCGTTAACCACCTG-3′ (the *Bsa*AI site is underlined, the TAV sequence is written in bold and the CMV sequence in regular type). The *Bam*HI and *Bsa*AI fragment of the PCR product was ligated into the pT3/BN clone digested with *Bam*HI and *Bsa*AI (nt 949–954) to create the clone pT3BSCMP. The *Nde*I–*Pst*I region of this clone was exchanged for the corresponding CMV region, resulting in the clone pTR3BSCMP (Fig. 1).

The chimeric CP clones (pT3SPR, pT3NSR, pR3NST and pR3SPT) were constructed using the *Nde*I and *Spe*I sites and the *Pst*I site located at the 3′ end of all the clones (Fig. 1).

PCR-directed mutagenesis was employed to change the sequences encoding Glu-62 and Lys-65 to Lys-62 and Arg-65, respectively, and to introduce a *Bam*HI restriction site into pR3/*Nde*I. The two primers used were 5′-GGGGATCCAAGAGCTGTAGACCCGGTTACAC-3′ and 5′-GGGGATCCCACGAAGGTTGGGTGG-3′ (mutated nucleotides are underlined). The *Nde*I–*Spe*I fragment was verified by DNA sequencing, then subcloned into the chimeras pT3NSR and pR3SPT resulting in the mutants pT3NSR62K65R and pR3SPT62K65R, respectively (Fig. 1). All RNA 3 clones were linearized with *Pst*I prior to *in vitro* transcription.

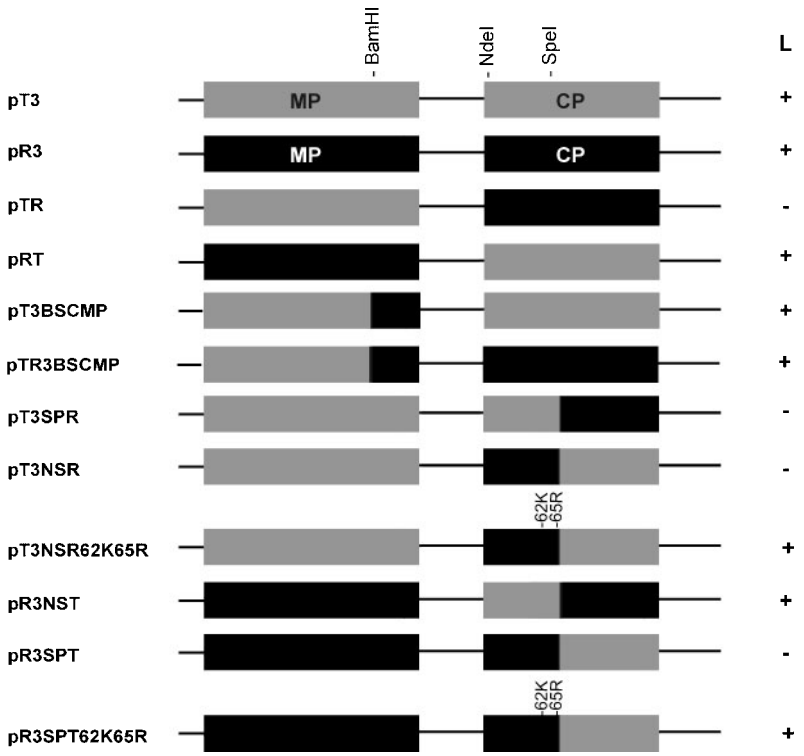

Fig. 1. Schematic representation of the wild-type RNA 3 cDNA construct and the RNA 3 constructs analysed in this study. Grey and black rectangles represent the genes originating from TAV and CMV, respectively. The MP and CP are indicated. Their ability to induce local infection in *N. clevelandii* plants is also indicated (L). +/−, Presence/absence of viral RNAs.

Plant inoculation. Plants (*Nicotiana* spp. and *Chenopodium* spp.) were inoculated at the three-leaf (*N. benthamiana*) or six-leaf (*N. clevelandii*, *C. quinoa*, *C. amaranticolor*) stage. The constructs were transcribed *in vitro* with T7 RNA polymerase. For inoculation, 2 μg of each of the RNA 1, 2 and 3 transcripts were used per plant in 50 μl 50 mM Na_2HPO_4, pH 8·6. Chimeric and mutated viruses were tested under confinement conditions in accordance with national regulations.

Preparation and transfection of tobacco protoplasts. Protoplasts were isolated from fully expanded *N. clevelandii* leaves and purified in K3 medium containing 0·4 M sucrose, based on the protocol of Nagy & Maliga (1976). Protoplast transfection with RNA transcripts was carried out as described by Kroner & Ahlquist (1992).

Analysis of plants and protoplasts. Total RNAs were extracted from the protoplasts 24 h after infection or from 200 mg fresh leaf tissue 6 days (inoculated leaves) and 14–21 days (systemic leaves) after inoculation (White & Kaper, 1989). Approximately 100 ng RNA was denatured with formaldehyde and formamide, electrophoresed in formaldehyde-containing agarose gels and blotted on to nylon membranes (Sambrook *et al.*, 1989). Northern blot hybridization analysis was performed with random-primed ^{32}P-labelled DNA fragments specific for the CMV or TAV sequences encoding the MP or CP, excised from pT3 or pR3 as described previously (Salánki *et al.*, 1997).

The method described by Lot *et al.* (1972) was used for virion purification. RNA was extracted from virions with phenol and SDS. First-strand cDNA was synthesized using CMV or TAV 3′-end-specific primers and avian myeloblastosis virus reverse transcriptase. PCR amplification was carried out with the 3′-end-specific primer containing a *Pst*I recognition site and 5′-specific primers containing a *Bam*HI recognition site using *Pfu* DNA polymerase. After digestion with *Bam*HI and *Pst*I, the PCR product was cloned into the pUC19 vector. The fragments of interest were verified by automated dideoxy-sequencing.

Sequence alignment, homology modelling, model refinement, electrostatic computation and structure evaluation of the CPs. Protein models were constructed employing the MODELLER 6.1 program (Sali, 1995). Five models have been generated using the subunit B of Fny-CMV coat protein (PDB ID code 1F15) as the template structure (Smith *et al.*, 2000). All models contain 190 residues from residue 29 to 218 corresponding to the B chain of the template coat protein. Sequence alignments and similarity values were calculated using the Wisconsin Package Version 10.0. Both the R-CMV CP and the P-TAV CP contain 218 residues and the sequence analyses showed high levels of homology. The sequences appear in the EMBL/GenBank/DDBF databases under accession numbers Y18138 and L15335 for the R-CMV CP and the P-TAV CP, respectively. The models were refined with energy minimization using a molecular mechanics force field (Kollman-All-Atom with Kollman charges; Weiner *et al.*, 1984) incorporated in the SYBYL 6.5 software package 1998. At the beginning of the energy minimization, the steepest descent technique was used to eliminate the steric conflicts between the side-chain atoms until the root mean square (rms) force reached 50 kcal mol^{-1} Å^{-1}. Reaching this threshold, the program automatically continued the energy minimization performing Powell conjugate gradient optimization until the maximum derivate became less than 0·05 kcal mol^{-1} Å^{-1}. We applied a distance-dependent dielectric constant (ε=4R). The atomic charges for all atoms were obtained from the Kollman-All-Atom force field. Electrostatic potential maps were calculated by the linearized Poisson–Boltzmann method (Gilson *et al.*, 1987) using a dielectric constant of 80 and 4·0 for the water solvent and protein core, respectively. The ionic strength was fixed at 0·1 mol l^{-1}. All Lys (+1), Arg (+1), Glu (−1) and Asp (−1) side chains were considered as ionized (actual charges in parentheses). Atomic charges were calculated using the GRASP program (Nicholls *et al.*, 1991). Molecular graphics and the electrostatic potential representations were created by the Swiss PDB Viewer 3.7 (Guex & Peitsch, 1997) using GRASP surface files with electrostatic property.

Evaluation of the refined models was carried out with PROCHECK (Laskowski *et al.*, 1993) and Swiss PDB Viewer 3.7.

RESULTS AND DISCUSSION

Construction of RNA 3 chimeras and their infectivity in *N. clevelandii* protoplasts

Prior to the generation of chimeric RNA 3 clones, restriction endonuclease recognition sites were introduced into the same position in pT3/NdeI and pR3/NdeI by silent mutagenesis. For the MP, the locations of the exchange points were defined after considering the results of Nagano *et al.* (1997). The CMV MP can assist cell-to-cell movement in the presence of *Brome mosaic virus* (BMV) CP if the C-terminal 33 aa of the MP are absent. Of these 33 aa, the N-terminal three were identical in CMV and TAV. Thus, we focused on the C-terminal 30 aa of the MP. A *Bam*HI restriction site was introduced by mutagenesis into the nucleotide sequence of pT3/NdeI corresponding to aa 248–250 of the MP. This mutation was silent and allowed the exchange of sequences encoding the C-terminal 30 aa of TAV for those encoding the 29 aa of CMV (the amino acid corresponding to aa 272 of TAV MP is absent in CMV MP).

The sites of exchange for the CP were designed based on amino acid sequence similarity. Comparison of the amino acid sequences of the CMV and TAV CP revealed higher dissimilarity in the N-terminal part of the protein (40·58 % identity for the N-terminal 70 aa and 63·33 % identity for the C-terminal 149 aa). An *Spe*I restriction endonuclease recognition site was introduced by mutagenesis into the CPs of pT3/NdeI and pR3/NdeI at aa 149.

The infectivity of the *Bam*HI and *Spe*I silent mutants was tested in the presence of pR1 and pR2 transcripts in *C. quinoa*, *N. benthamiana* and *N. clevelandii* plants. The infection phenotypes of the mutated clones were identical to the original pT3 or pR3 (data not shown).

Using the above-described restriction sites, various RNA 3 chimeras were constructed. The chimeric MP encoded the first 250 aa of TAV fused to the C-terminal 29 aa of CMV. Constructs contained this MP sequence in combination with either the TAV (pT3BSCMP) or the CMV (pTR3BSCMP) CP. Viruses containing a chimeric CP composed of the N-terminal 69 aa of TAV and the C-terminal 150 aa of CMV were combined with both the TAV (pT3SPR) and the CMV (pR3NST) MP. The reciprocal CP construct containing the 69 aa of CMV followed by 150 aa of TAV also was incorporated into clones containing either the TAV (pT3NSR) or the CMV (pR3SPT) MP (Fig. 1).

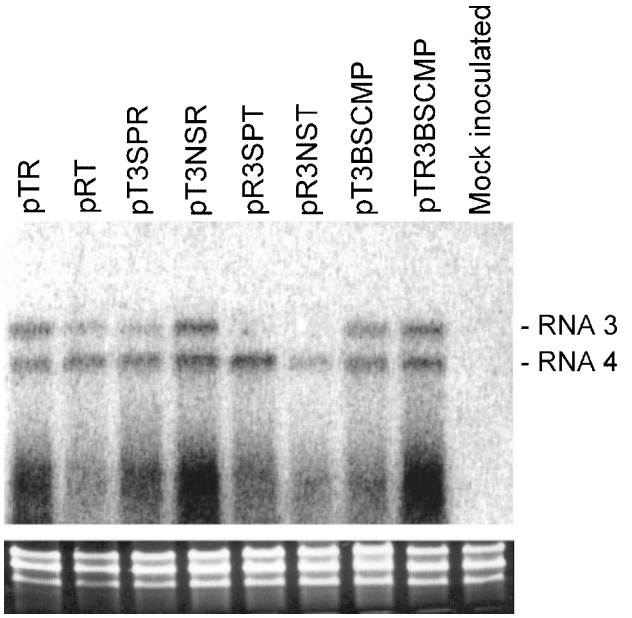

Fig. 2. Progeny analysis of *N. clevelandii* protoplasts inoculated with the *in vitro* transcripts of different chimeras in the presence of pR1 and pR2 transcripts. The radiolabelled probe was specific to CMV and TAV CP. Ethidium bromide-stained rRNA from the same volume of each sample is shown below each lane.

The replication ability of the different RNA 3 chimeras, co-inoculated with pR1 and pR2 *in vitro* transcripts, was examined in *N. clevelandii* protoplasts. The chimeras replicated efficiently except for pR3SPT and pR3NST. For these two constructs, the RNA 3 accumulation was significantly lower than for the other constructs; however, RNA 4 accumulated to a level comparable with the other constructs (Fig. 2).

Infectivity of the MP chimeras

Several common hosts of CMV and TAV (*N. clevelandii*, *N. benthamiana*, *C. quinoa* and *C. amaranticolor*) were inoculated with *in vitro* transcripts of the different chimeric and control RNA 3 clones in the presence of the R1 and R2 transcripts. All inoculation experiments were carried out at least three times and the results of the infections were consistent (see Table 1).

Replacing the C-terminal 30 aa of the TAV MP with the homologous 29 aa of CMV in pT3 (pT3BSCMP) did not abolish infectivity of the chimeric virus. However, the symptoms appeared later and were milder on all tested host plants compared with the parental virus (Table 1). This suggested that, although the chimeric MP was functioning, its structure was not optimal.

As this chimeric MP (TAV MP replaced with the C-terminal 30 amino acids replaced with the 29 amino acids of the CMV MP) enabled virus movement, it was used to replace the MP of the movement-deficient pTR, producing pTR3BSCMP. The movement of the virus was restored, although the appearance of symptoms was delayed, as was observed for the infection involving pT3BSCMP (Table 1). Northern blot hybridization analysis confirmed the presence and identity of the chimeric viruses (Fig. 3).

The C terminus of the CMV MP proved to be less specific than the corresponding region of the TAV MP, since it

Table 1. Assay of infectivity of parental and chimeric viruses

	Northern blot hybridization analysis*		Symptoms†		
	Protoplast	Inoculated leaf	Local	Systemic	
			Chenopodium spp.‡	*N. clevelandii*	*N. benthamiana*
pT3	+	+	Lesions	Mosaic	Mosaic, stunting
pR3	+	+	Lesions	Mosaic	Mosaic, stunting
pTR	+	−	−	−	−
pRT	+	+	Lesions	Mosaic	Mosaic, stunting
pT3BSCMP	+	+	Lesions	Mild, delayed mosaic	Mild, delayed mosaic and stunting
pTR3BSCMP	+	+	Lesions	Mild, delayed mosaic	Mild, delayed mosaic and stunting
pT3NSR	+	−	−	−	−
pT3SPR	+	−	−	−	−
pR3SPT	+	−	−	−	−
pR3NST	+	+	Lesions	Mosaic	Mosaic, stunting

*+/−, Presence/absence of viral RNA in protoplasts or inoculated leaves of *Nicotiana clevelandii*.

†−, no symptoms.

‡*Chenopodium quinoa*, *C. amaranticolor*.

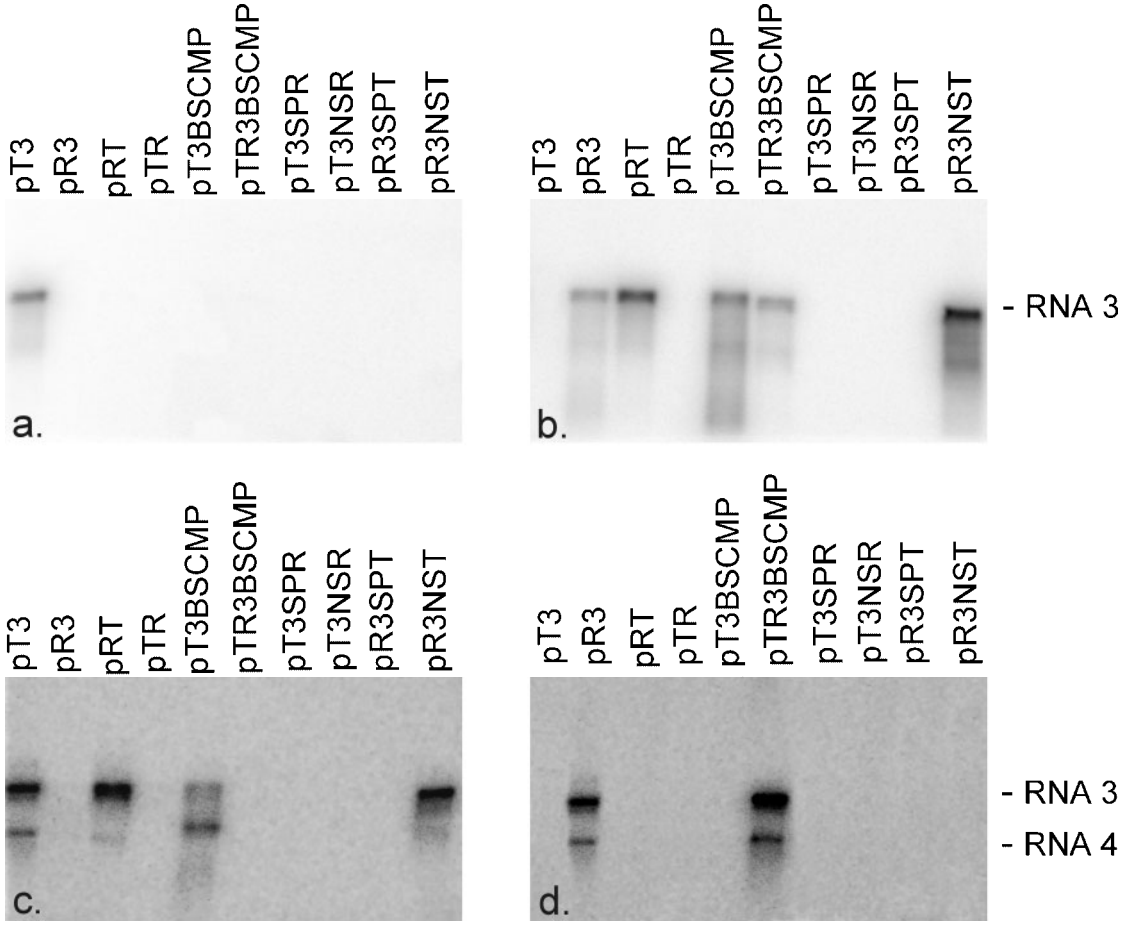

Fig. 3. Northern blot hybridization analysis of inoculated *N. clevelandii* leaves. *In vitro* RNA transcripts of each construct were co-inoculated with cDNA-derived transcripts of R-CMV RNA 1 and 2. The radiolabelled probe was specific to the 3′-terminal 90 nt of the TAV MP coding region (a), the 3′-terminal 90 nt of the CMV MP coding region (b), the 5′-terminal 210 nt of the TAV CP coding region (c) and the 5′-terminal 210 nt of the CMV CP coding region (d). RNAs 3 and 4 are indicated.

enabled cell-to-cell movement in the presence of both CMV and TAV CP, while this region of the TAV MP could assist this process only in the presence of homologous CP. In the case of cucumoviruses, similar incompatibility was reported for RNA 1 and 2 of CMV and PSV. While PSV RNA 1 replicated with both CMV and PSV RNA 2, the CMV RNA 1 and PSV RNA 2 could not function together (Suzuki *et al.*, 2003).

No specific domains necessary for movement functions (RNA binding, incorporation into the plasmodesmata, promoting cell-to-cell movement) have been identified in the exchanged 29 aa (Li *et al.*, 2001). According to Nagano *et al.* (1997), the 33 aa C-terminal part of the CMV MP determined whether the CP was required for movement. If this region was missing, movement occurred in a CP-independent manner. C-terminal deletions ranging from 31 to 36 aa of the MP also promoted virus cell-to-cell movement independent of viral CP (Nagano *et al.*, 2001). Our results confirm the role of the C-terminal 29 aa in the requirement for specific CP sequences, but not of the preceding region, because the specificity of the protein was already changed by altering the C-terminal 29 aa.

The C-terminal region of viral MPs has also been shown to provide specificity to the transport process in several other virus groups, for example in the case of the *Alfalfa mosaic virus* (Sánchez-Navarro & Bol, 2001), *Potato virus X* (Morozov *et al.*, 1999) and tobamoviruses (Fenczik *et al.*, 1995), but the mechanism mediating this specificity has not yet been determined.

The infectivity of the CP chimeras

To determine the CP region contributing to MP specificity, transcripts of CP chimeric constructs (pT3SPR, pT3NSR, pR3NST and pR3SPT) were inoculated in the presence of R1 and R2 transcripts. Visible symptoms appeared only on the plants co-inoculated with the construct pR3NST (Table 1). Northern blot hybridization analysis of the infected leaves confirmed the visual observations and the identity of the R3NST virus (Fig. 3). Even though the pT3SPR, the

pT3NSR and the pR3SPT constructs replicated in *N. clevelandii* protoplasts (Fig. 2), no viral RNA was detected either in the inoculated (Fig. 3) or in the upper leaves of the different *Nicotiana* species. No signs of infection were observed on the infected plants, even 6 weeks after inoculation.

The non-infectious pT3SPR construct has the same CP organization as the infectious pR3NST construct, showing that this CP was able to provide its essential functions and promote virus movement if combined with the appropriate MP. The cell-to-cell movement of the non-infectious TR virus could not be restored by changing the N-terminal 70 aa for the corresponding TAV region (pT3SPR). The inability of the pT3SPR construct to move from cell to cell indicates an altered interaction of the different viral proteins, principally the MP of TAV and the chimeric CP.

The chimeric CP construct encoding the N-terminal region of CMV and the C-terminal part of TAV was not infectious, either in combination with the TAV MP (pT3NSR) or with the CMV MP (pR3SPT); however, the CMV MP was able to promote the cell-to-cell movement of the viruses in the presence of either the CMV or the TAV CP. This result indicated that the above-described chimeric CP could not ensure the functions necessary for virus movement. This deficiency could derive from the structural changes resulting from the construction. To explain this phenomenon, further analysis of the different CP structures was conducted.

Computer analysis of the CPs

When the CP homology models were constructed, only the X-ray structure of Fny-CMV CP was available (Smith *et al.*, 2000). The model structure of the P-TAV CP was created to be used as a reference structure in further experiments. This P-TAV CP model fits excellently with 1·25 Å rms deviation to the B-chain of the B-TAV CP that was published subsequently (Lucas *et al.*, 2002). The models of the chimeric CPs were constructed to recognize the structural changes caused by the chimeric nature of the protein.

The reliability of the models is demonstrated in Table 2. The CP model structure of the movement-deficient construct (the CP of pR3SPT and pT3NSR) was compared with the structure of all other constructs (P-TAV CP, R-CMV CP, pR3NST CP), but no significant differences were recognized. For in-depth examination of the CP surface properties, electrostatic potential analysis was carried out based on the models.

The analysis of structures of the CP models revealed two pockets on the surface located between the first coil region after the N-terminal α-helix and behind the 'jelly roll' β-barrel domain (B, I, D, G β strands; Fig. 4A). A contact zone was identified between the coil region and the 'jelly roll' domain fixed to each other by H-bonds. The pockets evolved on both sides of this contact zone. In the X-ray structure of the TAV CP (Blencowe strain, PDB ID code 1LAJ; Lucas *et al.*, 2002), the previously described two pockets could also be found and were even connected by a channel. The size of the observed pockets was determined to be 9 Å and 11 Å with the assistance of the CASTp program (Liang *et al.*, 1998).

Differences between the infectious and non-infectious constructs were identified in this area. In the infectious constructs (P-TAV, R-CMV and R3NST), the electrostatic potential around aa 62 of the CP was predominantly positive, even if a slight negative potential at the bottom of the pocket of R-CMV also appeared (Fig. 4D). In the movement-deficient pR3SPT CP construct, there were two residues (Glu-62 and Lys-65) contributing to the negative electrostatic potential (the Glu-62 carboxylate group and the Lys-65 amide amino group) in this contact zone. In R-CMV CP, the same residues were located at these positions (Glu-62 and Lys-65). The comparison of the two CPs (pR3SPT and R-CMV CP) having negative electrostatic potential values in this region (Fig. 4D and F) showed that the negative charge of Glu-62 influenced a much larger area on the molecular surface of pR3SPT CP (Fig. 4F) than R-CMV CP (Fig. 4D). Similarly, the positive charge of Lys-65 impacted a much smaller area on the surface of

Table 2. Quality of CP structures refined by the SYBYL program

Ramachandran plot qualities show the percentage of residues belonging to the allowed, generally allowed and disallowed region of the plot. Goodness factors show the quality of the covalent and overall bond/angle distances. These scores should be above −0·50 for a reliable model. The rms deviation values show the overall difference between 3D models and the template.

Refined model	Ramachandran plot quality (%)			Goodness factors		Rms deviation from template backbone (Å)
	Allowed	General	Disallowed	Covalent	Total	
FNY-CMV CP (template)	95·2	1·8	3·0	−0·02	−0·18	–
pT3 (P-TAV) CP	98·2	0·6	1·2	0·33	−0·09	0·83
pR3 (R-CMV) CP	98·2	0·6	1·2	0·37	−0·10	0·77
pR3NST and pT3SPR CP	97·7	0·6	1·8	0·37	−0·11	0·75
pR3SPT and pT3NSR CP	98·7	0·6	0·6	0·34	−0·07	0·83
pR3SPT62K65R and pT3NSR62K65R CP	98·1	0·6	1·2	0·34	−0·07	0·76

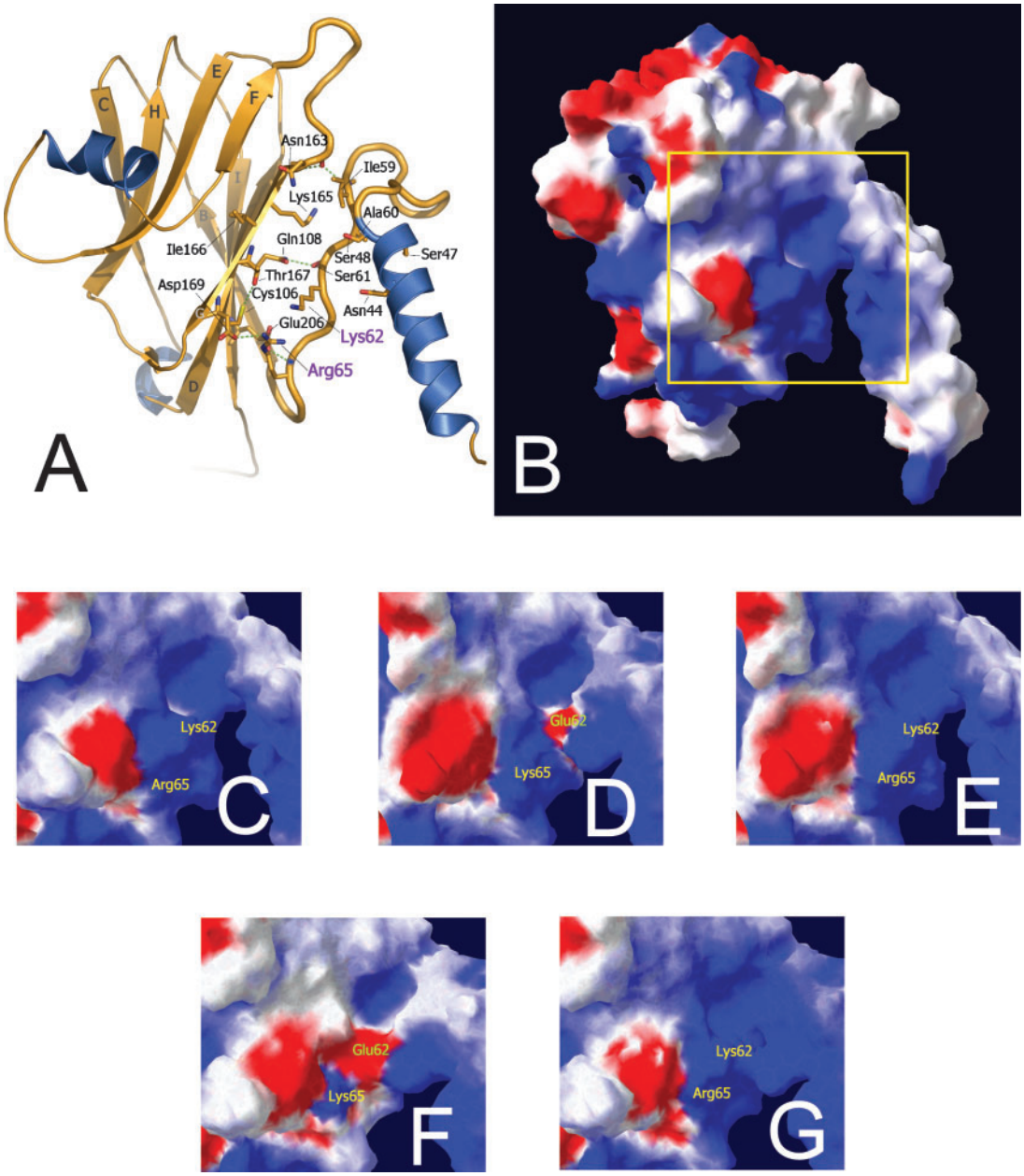

Fig. 4. Analysis of the CP structure. (A) Detailed backbone conformation of the B subunit P-TAV CP model with β-sheet labelling. The side chains of the residues are coloured according to atom type: nitrogen atoms are blue, carbon atoms are orange, oxygen atoms are red and the sulfur atom is yellow. The green broken lines show H-bonds. The picture was produced by PyMol (available at http://www.pymol.org). (B) Electrostatic view of the P-TAV CP B subunit molecular surface. The region scrutinized for the following CP constructs is framed: P-TAV CP (C), R-CMV CP (D), pR3NST CP (E), pR3SPT CP (F) and pR3SPT62K65R CP (G). Red, regions with potential value less than −1·8 kT; white, 0·0; blue, greater than +1·8 kT. Amino acids 62 and 65 are indicated in (A) and (C–G).

pR3SPT CP (Fig. 4F) than on R-CMV CP (Fig. 4D). The dissimilarities in the charge distribution of the molecule surfaces can be explained by differences in the conformation of these and the surrounding residues.

Presumably, in the case of pR3SPT CP there was no electrostatic complementarity (Náray-Szabó, 1993) required for successful interaction with other viral and/or host proteins (Fig. 4F) and this was the reason for the movement deficiency of this construct. A double mutation was designed to modify the electrostatic potential pattern of this CP construct. Residues Glu-62 and Lys-65 were changed to Lys and Arg, respectively, to mimic the P-TAV CP residues Lys-62 and Arg-65. The mutated clone was referred to as

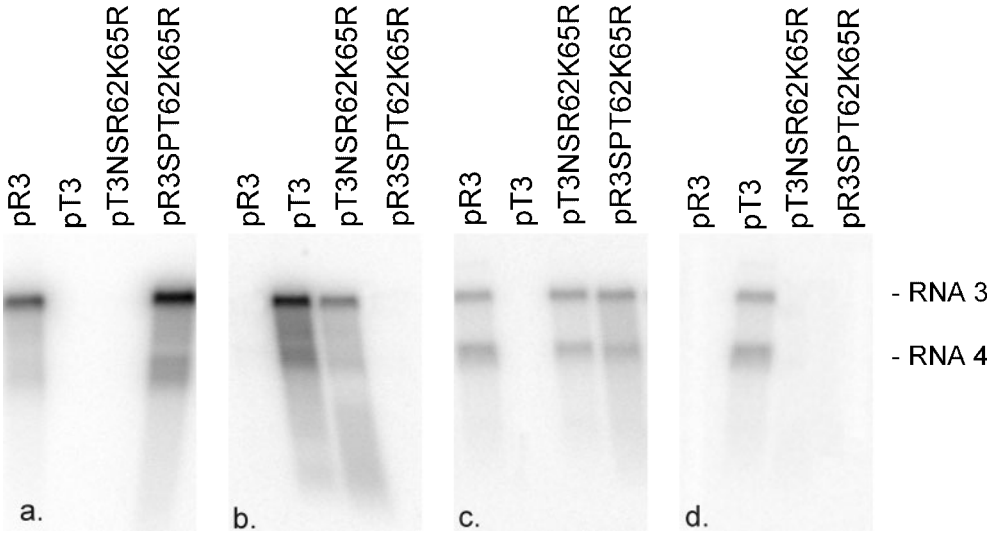

Fig. 5. Northern blot hybridization analysis of viral RNA in inoculated leaves of *N. clevelandii* plants. Total nucleic acids were extracted from the leaves of tobacco plants inoculated with *in vitro* transcripts from cDNA clones of R-CMV RNAs 1 and 2 together with *in vitro* transcripts from cDNA clones of the chimeric RNA 3 constructs. The radiolabelled probe was specific to the 3′-terminal 90 nt of the CMV MP coding region (a), the 3′-terminal 90 nt of the TAV MP coding region (b), the 5′-terminal 210 nt of the CMV CP coding region (c) and the 5′-terminal 210 nt of the TAV CP coding region (d). RNAs 3 and 4 are indicated.

pR3SPT62K65R. As a result, the electrostatic pattern of the contact zone of pR3SPT62K65R became similar to those of the other infectious constructs (Fig. 4G).

Analysis of the R3SPT62K65R and T3NSR62K65R mutants

Different *Chenopodium* and *Nicotiana* species were inoculated with *in vitro* transcripts of pR3SPT62K65R together with those of the pR1 and pR2 clones. In the case of the mutant chimeric virus, local lesions appeared 7 days post-inoculation on the *Chenopodium* species. Systemic symptoms on different *Nicotiana* plants appeared 10 days post-inoculation (data not shown). Northern blot hybridization analysis of the inoculated leaves confirmed the visual observations (Fig. 5). The virus R1R2R3SPT62K65R was purified and the identity of the engineered mutation was confirmed by nucleotide sequence determination after cDNA synthesis and PCR amplification. The determined sequence was identical to the sequence of the corresponding infectious clone (data not shown).

These results drew our attention to the region surrounding aa 62–65 of the CP where a potential protein binding site was predicted. Two questions arose about this region of the CP: (i) whether both of the above-described pockets function as real binding sites, forming a dimer or trimer macromolecular complex; and (ii) what could be binding to this region of the CP? The latter could be one of the viral proteins, a plant protein or a plant co-factor. The movement-deficient CP could not promote cell-to-cell movement, with either the TAV MP (T3NSR) or with the CMV MP (R3SPT). This indicated that the region surrounding aa 62–65 of the CP did not contribute to the MP specificity, but had some other essential role in cell-to-cell movement.

This part of the CP did not belong to any of the functional domains identified so far. The regions required for particle assembly were identified at the N-terminal end of the CP. Crucial amino acids for particle assembly were located in the first 19 residues (Schmitz & Rao, 1998) and between the 15th and 40th amino acid (Kaplan *et al.*, 1998). Residues 129 (Suzuki *et al.*, 1995; Shintaku *et al.*, 1992; Perry *et al.*, 1994, 1998) and 193 (Szilassy *et al.*, 1999), identified as being responsible for symptom induction and/or aphid transmission, were also located elsewhere on the CP.

The importance not only of the specific amino acid, but also of the surface domain conservation was demonstrated recently by Liu *et al.* (2002) who investigated the role of the βH–βI loop in aphid transmission.

As the infectivity of the chimeric CP was restored by two mutations, the CP of the movement-deficient TR clone was replaced by this chimeric CP resulting in clone pT3NSR62K65R. *Nicotiana* and *Chenopodium* species were infected with the *in vitro* transcripts of pT3NSR62K65R, pR1 and pR2. Symptoms appeared on all inoculated plants and Northern blot hybridization analysis confirmed the presence of the virus (Fig. 5). The virus was purified and the RNA 3 cloned. The nucleotide sequence determination confirmed the identity of the engineered mutation.

Replacing the C-terminal two-thirds of the CMV CP with the equivalent TAV region restored the infectivity of the TR virus, but only after mutation at CP residues 62 and 65 (pT3NSR62K65R). The TAV MP could promote cell-to-cell movement only if this part of the CP also originated from TAV. Taking this and the results of the experiments with the MP chimeras into account, the C-terminal two-thirds of the CP and the 29 aa-long C-terminal region of the MP of cucumoviruses need to be compatible to enable virus movement. Direct interaction between the MP and the CP has been observed in case of *Maize streak virus* (Liu *et al.*, 2001) and *Tomato spotted wilt virus* (Soellick *et al.*, 2000), but has not been reported for cucumoviruses.

A more precise identification of the region responsible for specificity is rather difficult, because the amino acid sequence of this region is diverse between TAV and CMV, even though the different amino acid sequences form quite similar 3D CP structures. The previously detailed 3D structural analysis will probably help to localize more precisely the region responsible for compatibility with the MP protein. The availability of the 3D structure of the MP would considerably facilitate identification of the compatible sections.

ACKNOWLEDGEMENTS

We are grateful to Dr Mark Tepfer and Dr Johannes VanStaden for critical reading of the manuscript. The work was supported by research grants OTKA T 032737, T 034994 and VRTP IMPACT QLK3-CT-2000-00361. K. S. received a Bolyai János Fellowship from the Hungarian Academy of Sciences. We thank Nádudvariné Júlia Novák for excellent technical assistance.

REFERENCES

Béclin, C., Berthome, R., Palauqui, J. C., Tepfer, M. & Vaucheret, H. (1998). Infection of tobacco or *Arabidopsis* plants by CMV counteracts systemic post-transcriptional silencing of nonviral (trans) genes. *Virology* **252**, 313–317.

Brigneti, G., Voinnet, O., Li, W. X., Ji, L. H., Ding, S. W. & Baulcombe, D. C. (1998). Viral pathogenicity determinants are suppressors of transgene silencing in *Nicotiana benthamiana*. *EMBO J* **17**, 6739–6746.

Carrington, J. C., Kasschau, K. D., Mahajan, S. K. & Schaad, M. C. (1996). Cell-to-cell and long-distance transport of viruses in plants. *Plant Cell* **8**, 1669–1681.

Cooper, B. & Dodds, J. A. (1995). Differences in the subcellular localization of tobacco mosaic virus and cucumber mosaic virus movement proteins in infected and transgenic plants. *J Gen Virol* **76**, 3217–3221.

Ding, B., Li, Q., Nguyen, L., Palukaitis, P. & Lucas, W. J. (1995). Cucumber mosaic virus 3a protein potentiates cell-to-cell trafficking of CMV RNA in tobacco plants. *Virology* **10**, 345–353.

Ding, S. W., Shi, B. J., Li, W. X. & Symons, R. H. (1996). An interspecies hybrid RNA virus is significantly more virulent than either parental virus. *Proc Natl Acad Sci U S A* **93**, 7470–7474.

Fenczik, C. A., Padgett, H. S., Holt, C. A., Casper, S. J. & Beachy, R. N. (1995). Mutational analysis of the movement protein of odontoglossum ringspot virus to identify a host-range determinant. *Mol Plant Microbe Interact* **8**, 666–673.

Gilson, M. K., Sharp, K. A. & Honig, B. (1987). Calculating electrostatic interactions in biomolecules: method and error assessment. *J Comp Chem* **9**, 327–335.

Guex, N. & Peitsch, M. C. (1997). SWISS-MODEL and the Swiss-PdbViewer: an environment for comparative protein modeling. *Electrophoresis* **18**, 2714–2723.

Huppert, E., Szilassy, D., Salánki, K., Divéki, Z. & Balázs, E. (2002). Heterologous movement protein strongly modifies the infection phenotype of cucumber mosaic virus. *J Virol* **76**, 3554–3557.

Kaplan, I. B., Shintaku, M. H., Li, Q., Zhang, L., Marsh, L. E. & Palukaitis, P. (1995). Complementation of virus movement in transgenic tobacco expressing the cucumber mosaic virus 3a gene. *Virology* **10**, 188–199.

Kaplan, I. B., Zhang, L. & Palukaitis, P. (1998). Characterization of cucumber mosaic virus. V. Cell-to-cell movement requires capsid protein but not virions. *Virology* **5**, 221–231.

Kroner, P. & Ahlquist, P. (1992). RNA-based viruses. In *Molecular Plant Pathology. A Practical Approach*, vol. I, pp. 23–34. Oxford: IRL Press.

Laskowski, R. A., MacArthur, M. W., Moss, D. S. & Thornton, J. M. (1993). PROCHECK: a program to check the stereochemical quality of protein structures. *J Appl Cryst* **26**, 283–291.

Lazarowitz, S. G. & Beachy, R. N. (1999). Viral movement proteins as probes for intracellular and intercellular trafficking in plants. *Plant Cell* **11**, 535–548.

Li, Q. & Palukaitis, P. (1996). Comparison of the nucleic acid- and NTP-binding properties of the movement protein of cucumber mosaic cucumovirus and tobacco mosaic tobamovirus. *Virology* **216**, 71–79.

Li, Q., Ryu, K. H. & Palukaitis, P. (2001). Cucumber mosaic virus–plant interactions: identification of 3a protein sequences affecting infectivity, cell-to-cell movement, and long-distance movement. *Mol Plant Microbe Interact* **14**, 378–385.

Liang, J., Edelsbrunner, H. & Woodward, C. (1998). Anatomy of protein pockets and cavities: measurement of binding site geometry and implications for ligand design. *Protein Sci* **7**, 1884–1897.

Liu, H., Boulton, M. I., Oparka, K. J. & Davies, J. W. (2001). Interaction of the movement and coat proteins of *Maize streak virus*: implications for the transport of viral DNA. *J Gen Virol* **82**, 35–44.

Liu, S., He, X., Park, G., Josefsson, C. & Perry, K. L. (2002). A conserved capsid protein surface domain of *Cucumber mosaic virus* is essential for efficient aphid vector transmission. *J Virol* **76**, 9756–9762.

Lot, H., Marrou, J., Quiot, J. B. & Esvan, C. (1972). Contribution á l'étude du virus de la mosaique du concombre (CMV). I. Méthode de purification rapide du virus. *Ann Phytopath* **4**, 25–38.

Lucas, R. W., Steven, B. L., Canady, M. A. & McPherson, A. (2002). The structure of tomato aspermy virus by X-ray crystallography. *J Struct Biol* **139**, 90–102.

Melcher, U. (1990). Similarities between putative transport proteins of plant viruses. *J Gen Virol* **71**, 1009–1018.

Morozov, S. Y., Solovyev, A. G., Kalinina, N. O., Fedorkin, O. N., Samuilova, O. V., Schiemann, J. & Atabekov, J. G. (1999). Evidence for two nonoverlapping functional domains in the potato virus X 25K movement protein. *Virology* **260**, 55–63.

Nagano, H., Okuno, T., Mise, K. & Furusawa, I. (1997). Deletion of the C-terminal 33 amino acids of cucumber mosaic virus movement protein enables a chimeric brome mosaic virus to move from cell to cell. *J Virol* **71**, 2270–2276.

Nagano, H., Mise, K., Furusawa, I. & Okuno, T. (2001). Conversion in the requirement of coat protein in cell-to-cell movement mediated by the cucumber mosaic virus movement protein. *J Virol* **75**, 8045–8053.

Nagy, J. I. & Maliga, P. (1976). Callus induction and plant regeneration from mesophyll protoplasts of *Nicotiana sylvestris*. *Z Pflanzenphysiol* **78**, 453–455.

Náray-Szabó, G. (1993). Analysis of molecular recognition: steric electrostatic and hydrophobic complementarity. *J Mol Recognit* **6**, 205–210.

Nicholls, A., Sharp, K. & Honig, B. (1991). Protein folding and association – insights from the interfacial and thermodynamic properties of hydrocarbons. *Proteins Struct Funct Genet* **11**, 281–296.

Nitta, N., Takanami, Z., Kuwata, S. & Kubo, S. (1988). Inoculation with RNAs 1 and 2 of cucumber mosaic virus induces viral RNA replicase activity in tobacco mesophyll protoplasts. *J Gen Virol* **69**, 2695–2700.

Perry, K. L., Zhang, L., Shintaku, M. H. & Palukaitis, P. (1994). Mapping determinants in cucumber mosaic virus for transmission by *Aphis gossypii*. *Virology* **205**, 591–595.

Perry, K. L., Zhang, L. & Palukaitis, P. (1998). Amino acid changes in the coat protein of cucumber mosaic virus differentially affect transmission by the aphids *Myzus persicae* and *Aphis gossypii*. *Virology* **242**, 204–210.

Ryabov, E. V., Roberts, I. M., Palukaitis, P. & Taliansky, M. (1999). Host-specific cell-to-cell and long-distance movements of cucumber mosaic virus are facilitated by the movement protein of groundnut rosette virus. *Virology* **260**, 98–108.

Salánki, K., Balázs, E. & Burgyán, J. (1994). Nucleotide sequence and infectious in vitro transcripts of RNA 3 of tomato aspermy virus pepper isolate. *Virus Res* **33**, 281–289.

Salánki, K., Carrere, I., Jacquemond, M., Balázs, E. & Tepfer, M. (1997). Biological properties of pseudorecombinant and recombinant strains created with cucumber mosaic virus and tomato aspermy virus. *J Virol* **71**, 3597–3602.

Sali, A. (1995). Modeling mutations and homologous proteins. *Curr Opin Biotechnol* **6**, 437–451.

Sambrook, J., Fritsch, E. F. & Maniatis, T. (1989). *Molecular Cloning: a Laboratory Manual*, 2nd edn. Cold Spring Harbor, NY: Cold Spring Harbor Laboratory.

Sánchez-Navarro, J. A. & Bol, J. F. (2001). Role of the alfalfa mosaic virus movement protein and coat protein in virus transport. *Mol Plant Microbe Interact* **14**, 1051–1062.

Schmitz, I. & Rao, A. L. (1998). Deletions in the conserved amino-terminal basic arm of cucumber mosaic virus coat protein disrupt virion assembly but do not abolish infectivity and cell-to-cell movement. *Virology* **248**, 323–331.

Shi, B. J., Miller, J., Symons, R. H. & Palukaitis, P. (2003). The 2b protein of cucumoviruses has a role in promoting the cell-to-cell movement of pseudorecombinant viruses. *Mol Plant Microbe Interact* **16**, 261–267.

Shintaku, M. H., Zhang, L. & Palukaitis, P. (1992). A single amino acid substitution in the coat protein of cucumber mosaic virus induces chlorosis in tobacco. *Plant Cell* **4**, 751–757.

Smith, T. J., Chase, E., Schmidt, T. & Perry, K. L. (2000). The structure of cucumber mosaic virus and comparison to cowpea chlorotic mottle virus. *J Virol* **74**, 7578–7586.

Soards, A. J., Murphy, A. M., Palukaitis, P. & Carr, J. P. (2002). Virulence and differential local and systemic spread of cucumber mosaic virus in tobacco are affected by the CMV 2b protein. *Mol Plant Microbe Interact* **15**, 647–653.

Soellick, T., Uhrig, J. F., Bucher, G. L., Kellmann, J. W. & Schreier, P. H. (2000). The movement protein NSm of tomato spotted wilt tospovirus (TSWV): RNA binding, interaction with the TSWV N protein, and identification of interacting plant proteins. *Proc Natl Acad Sci U S A* **97**, 2373–2378.

Suzuki, M., Kuwata, S., Kataoka, J., Masuta, C., Nitta, N. & Takanami, Y. (1991). Functional analysis of deletion mutants of cucumber mosaic virus RNA3 using an in vitro transcription system. *Virology* **183**, 106–113.

Suzuki, M., Kuwata, S., Masuta, C. & Takanami, Y. (1995). Point mutations in the coat protein of cucumber mosaic virus affect symptom expression and virion accumulation in tobacco. *J Gen Virol* **76**, 1791–1799.

Suzuki, M., Yoshida, M., Yoshinuma, T. & Hibi, T. (2003). Interaction of replicase components between cucumber mosaic virus and peanut stunt virus. *J Gen Virol* **84**, 1931–1939.

Szilassy, D., Salánki, K. & Balázs, E. (1999). Stunting induced by cucumber mosaic cucumovirus-infected *Nicotiana glutinosa* is determined by a single amino acid residue in the coat protein. *Mol Plant Microbe Interact* **12**, 1105–1113.

Vaquero, C., Turner, A. P., Demangeat, G., Sanz, A., Serra, M. T., Roberts, K. & Garcia-Luque, I. (1994). The 3a protein from cucumber mosaic virus increases the gating capacity of plasmodesmata in transgenic tobacco plants. *J Gen Virol* **75**, 3193–3197.

Vaquero, C., Sanz, A. I., Serra, M. T. & Garcia-Luque, I. (1996). Accumulation kinetics of CMV RNA 3-encoded proteins and subcellular localization of the 3a protein in infected and transgenic tobacco plants. *Arch Virol* **141**, 987–999.

Vaquero, C., Liao, Y. C., Nahring, J. & Fischer, R. (1997). Mapping of the RNA-binding domain of the cucumber mosaic virus movement protein. *J Gen Virol* **78**, 2095–2099.

Weiner, S. J., Kollman, P. A., Case, D. A. U., Singh, C., Ghio, C., Alagona, G., Profeta, S. & Weiner, P. (1984). A new force field for molecular mechanical simulation of nucleic acids and proteins. *J Am Chem Soc* **106**, 765–784.

White, J. L. & Kaper, J. M. (1989). A simple method for detection of viral satellite RNAs in small tissue samples. *J Virol Methods* **23**, 83–94.